LASER ABLATION AS A TOOL FOR ELEMENTAL AND ISOTOPIC SEPARATION: A PROSPECTIVE STUDY

Nicolau A.S. Rodrigues, Marcelo G. Destro, José W. Neri,
Rudimar Riva, Carlos A.B. Silveira, Carlos Schwab
Instituto de Estudos Avançados
Rodovia dos Tamoios km 5,5
12.228-970 – São José dos Campos
São Paulo – Brazil
nicolau@ieav.cta.br

Juliana B. Matos, Madalena A.P. Gião
Instituto Tecnológico de Aeronáutica
Praça Marechal Eduardo Gomes 50
12228-900 – São José dos Campos –
São Paulo - Brazil

Luiz V. Tarelho, Nilson D.Vieira Jr
Instituto de Pesquisas Energéticas e Nucleares
Av. Lineu Prestes 2242
São Paulo - Brazil

Abstract

Laser ablation has been widely used in analytical applications, such as, for instance, Laser Ablation Inductively Coupled Plasma Mass Spectrometry (LA-ICP-MS), because of their ability to remove material from solid samples and break part of the ablated material into its elementals. This aspect alone can already be viewed as a separation process. If laser ablation is combined with selective processes and devices, elemental separation can be done with resolution enough to be applied to isotopes. The combination of these two processes can be useful for elemental separation in applications where only tiny amounts of the products are desired. This paper suggests the use of laser ablation, combined with plasma traps and laser resonant ionization, as a tool for separation of virtually any material, taking solid complex samples as raw material.

Key Words: Laser ablation, Resonant laser ionization

1. Introduction

Since the advent of the ruby laser it is known that high intensity laser pulses can ablate solid targets[1]. Ever since, laser ablation has been widely used for Physical Vapor Deposition (PVD) [2, 3], Laser Induced Breakdown Spectroscopy (LIBS) [4], Inductively Coupled Plasma Mass Spectrometry (ICPMS) [5], material processing [6, 7] and many other applications. Initially ruby and CO_2 were used to produce and study laser ablation because they were the only lasers in the early times capable of producing pulses with intensity high enough to produce ablation [8, 9, 10]. Later, the excimer laser became widely used for ablation because, beside of the high intensity pulses, they emit in wavelengths shorter than the formerly used lasers [11]. Afterwards, the Nd-YAG and the femtosecond class lasers started to be studied in laser ablation applications [12]. In general, all these lasers have in common a high energy per pulse and low repetition rate. Recently, Chang reported the plume characterization of metals ablated by copper lasers in atmospheric air, aiming material processing [13] and Rodrigues reported ablation of refractory metals by using HyBrID lasers [14]. The main difference between copper laser and the others previously applied in laser ablation is that the copper laser emits low energy pulses at high repetition rate.

As far as laser ablation for isotope separation is concerned, Pronko reported boron isotope enrichment by using ablation of Boron Nitride (BN) targets with femtosecond lasers [15]. Singh presented results of unexpected isotope abundance in experiments of Boron ablation with Nd-YAG lasers in the range of nanosecond duration pulses [16]. In both cases the isotope separation is produced by the ablation itself.

Recently it was decided at IEAv to apply the facilities and know-how, obtained in uranium enrichment activities, to separate and enrich other isotopes than uranium, mainly those ones with interest in photonics [17], such as the rare earths, for instance. Different from the case of uranium, the enrichment of rare earth demands only tiny amounts of specific isotopes, mainly if they are desired for research activities. The installed lasers are easily adapted to the separation of rare earths. However, the same cannot be said about the evaporation facility. So, it was thought to use the same copper lasers (used to pump dye lasers) to produce the desired element vapor by using laser ablation.

This paper shows part of a study, in development yet, that aims to verify the feasibility of taking complex materials (such as monazitic sand, for instance), that contain a desired isotope, and separate the elements by laser ablation, for isotope separation purposes.

2. Laser ablation

Laser ablation is the general designation for the process of material removal due to the illumination of solid target surfaces by laser pulses. There are tree basic processes that lead to laser ablation: thermal evaporation, non-thermal evaporation and photo-dissociation [18-20]. The first case happens when a surface is heated by laser pulses with duration in the range of nanocosecond. The heat is transmitted to a very thin layer of material and, if the temperature is high enough to produce vapor, the vaporized material is spilled off with high velocity, very often dragging liquid portion of the target material. The non-thermal evaporation happens when femtosecond lasers are used. There is no time for heat transfer or thermalization and the heated surface is sublimated. The photo-dissociation happens with lasers in the ultra-violet. The vapor is produced by the breakage of molecules due to absorption of UV photons. This paper will concern only about the thermal evaporation process, and more specifically, the laser ablation of metals.

Capitelli presented a very extensive review with the description of the laser ablation and the plume expansion [21]. When a metal target is illuminated by laser pulses with duration τ, part of the pulse energy is absorbed basically by free electrons at the target surface which, due collisions with the matrix, lose energy to the bulk. The heat is dissipated due to thermal diffusion and a temperature gradient is formed with the surface temperature higher than the inner one. If a semi-infinite target is uniformly illuminated by a laser pulse, at the end of the pulse the temperature distribution along the z axis is given by [22]

$$\Delta T(z) = \frac{2aI}{K}(\kappa\tau)^{1/2}\,\mathrm{ierfc}\left[\frac{z}{L_D}\right] \quad (1)$$

$$\mathrm{ierfc}(x) = \int_x^\infty \mathrm{erfc}(s)\,ds \quad , \quad \mathrm{erfc}(x) = \left(\frac{2}{\pi}\right)^{1/2}\int_x^\infty e^{-s^2}\,ds$$

and $L_D = (4\kappa\tau)^{1/2}$.

L_D is the thermal diffusion length, that roughly indicates the heat penetration depth in the sample during the pulse duration; κ is the thermal diffusivity; K is the thermal conductivity; I is the power density; a is the absorption coefficient and z is the depth into the target.

If the laser pulse is intense and long enough, the surface temperature achieves the melting point and a liquid pool starts to travel inwards the target bulk. For even more intense and/or longer pulses, the surface can evaporate and even become a plasma. So, in ablation conditions, there is a heat front, followed by a liquid pool and by a vaporization front that travels to the interior of the target.

Let's take tungsten target illuminated by copper laser pulses. For the copper laser one has wavelength λ = 511 nm, pulse duration τ = 25 ns, pulse energy of about E = 1 mJ, a spot diameter of Φ = 25 μm, a peak power density of $I = 2\times10^9$ W/cm^2 and a a fluency (energy density) of ε = 5 J/cm^2. The tungsten thermal parameters can be obtained by averaging the values found in [22] between the room and boiling temperature. These values are: absorption coefficient a = 0.3 (at λ = 511 nm); thermal diffusivity κ = 0.4 cm^2/s and thermal conductivity of K = 12 W/cm °C. Substituting these values in 1-4, one has a thermal diffusion length of L_D = 2 μm and a surface temperature of ΔT = 8300 K. This surface temperature is much higher than the tungsten boiling temperature, so, it is reasonable to suppose that a layer thinner than L_D is evaporated and tends to expand outward the target surface, producing an expanding plume.

If the ablation is produced in vacuum, like in this work, the plume expanding velocity is in the order of 1000 m/s, as it will be seen ahead. Thus, at the end of the laser pulse, the vapor expands only about 25 μm. Supposing the vapor expansion occurs perpendicularly to the target surface, at the pulse end, the vapor density decreases only one order of magnitude from the solid density [13].

In short, the ablation of tungsten by copper laser can produce a vapor globule with very high temperature and very high pressures. In the specific case of metal ablation with copper vapor laser in atmosphere, Chang [6] found plume density in the early stages of the expansion, of 3×10^{20} - 1×10^{21} cm^{-3} , temperatures exceeding 1×10^4 K and expanding velocity of up to 6×10^3 m/s.

Just after the end of the laser pulse, the vapor with high temperature and pressure is highly collisional and in the very beginning of the plume expansion it quickly achieves thermal equilibrium [18]. So, it is expected that, at a distance much larger than L_D, the plume behaves like an expanding vapor in thermal equilibrium, with a drift velocity v_D. Due to the high temperature it is also reasonable to expect that the plume is highly ionized.

In order to consider the tlaser ablation in separation processes, it is necessary to answer some questions. Is the plume mainly monoatomic or poliatomic? Which is the fraction of the plume that is ionized? Since the plume temperature is very high, the Doppler effect can spoil any tentative of selective excitation, so, is the plume highly directional? If it is necessary to design a device to separate ions and electrons from the neutrals, what are the plasma characteristics? In order to answer these questions, it was accomplished an experimental study to evaluate the characteristics of a plume, produced by ablation of metal samples, using copper lasers. This paper presents these results.

3. Experimental setup

All the experiments in this work were accomplished using one basic setup configuration that is diagrammed in Fig. 1. The target is placed inside a vacuum chamber and illuminated by a copper laser beam, focused by a f = 200 mm BK7 lens. The laser beam strikes the target with an angle of 45° with the surface. The measuring devices that were used to characterize the plume are: mass spectrometer, PDVF pressure sensor, Langmuir probe and quartz oscillator

deposition rate sensor. The measurement devices characteristics will be discussed ahead in specific sections. Two different vacuum chambers were used, one with 100 liters and the other with 2 liters volume, both with a background pressure of 10^{-6}-10^{-5} mbar and having flanges for optical windows and feedthroughs.

During the first few laser pulses, the ablated plume jet is perpendicular to the target surface but, when holes are drilled in the target surfaces, the plume starts to follow the laser beam. So, to prevent holes formation (cratering), the target support is attached to a rotating feed-through (50 rpm) and the laser beam spot is slightly moved radially between two successive measurements.

Cooper lasers were used to ablate metal targets because of two main reasons: there are many copper lasers at IEAv due to the uranium enrichment program and it was already shown that the copper laser is able to produce small amount of vapor per pulse at high repetition rate [14], allowing good control on the evaporation rate. Two different copper lasers were used, with very similar characteristics: one copper vapor laser and one HyBrID copper laser [23], both built at IEAv. Table I shows the main laser characteristics. Only the green line was used in this work to prevent double focus due to chromatic aberration.

Table I: Laser parameters.

Characteristic	*Copper vapor laser*	*HyBrID copper laser*
Wavelength (nm)	512 (green), 578 (yellow)	
Pulse width (ns)	40-60	25-50
Repetition rate (kHz)	4-6	5-20
Pulse energy (mJ)	4	1
Peak power (kW)	80	30
Average power (W)	20	12
Beam quality (M^2)	32-60	4-6
Peak power density at the target surface	8×10^8 (W/cm^2)	5×10^8 (W/cm^2)

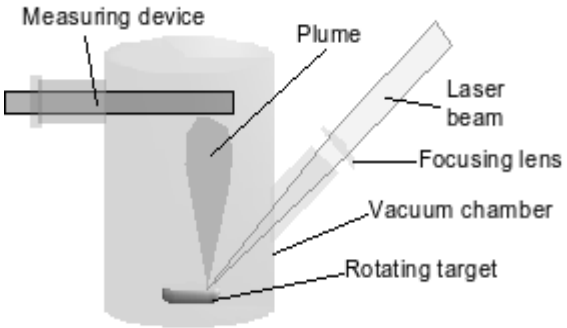

Figure 1: Basic experimental setup. A copper laser beam is focused on the surface of a target that is attached to a rotating feed-through. Depending on the measuring set, different measuring devices were used.

4. Mass spectrometer measurements

The first set of experiments was performed in order to verify the plume composition. A Pfeiffer mod. Prisma 300 mass spectromer was used to monitor the ions in the metal plumes. The spectrometer ion collector was put to intercept the plume 25 mm far from the target. This mass spectrometer is designed to analyze residual gas, thus it loses resolution when analyzing jets, anyway, it was used in the lack of a more adequate device. The mass spectrometer worked in two different regimes. In the first regime, the electron source that ionizes the vapor sample in the ion collector was turned off, such that any ion detected by the mass spectrometer was due exclusively to laser ablation. In the second regime the electron beam was turned on and the ions detected were due to laser ablation and to ionization of neutrals in the plume. Stainless steel, nickel, copper, tungsten and tantalum targets were analyzed. Fig. 2 shows a typical mass spectrum for stainless steel. Amoruso reported the observation of multi-ionization and cluster formation in experiments of copper ablation with XeF laser [24] Contrary to this author, we observed only singly ionized atoms and we didn't observe clusters either. Probably these results are due to the lack of resolution of our equipment, since we used an RGA mass spectrometer, as explained before. Nevertheless, our results allow us to conclude that most of the ionized particles (if not all) that composes the plume are monoatomic and singly ionized.

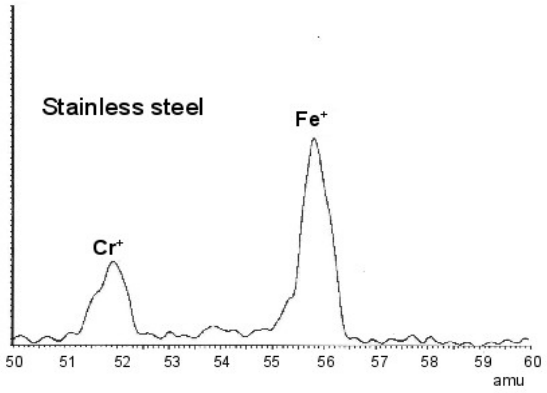

Figure 2: Mass spectrum obtained by ablating a stainless steel target. Only singly ionized monoatomic species were observed, within the device resolution.

5. PVDF sensor

The PVDF is a ferroelectric polymer that exhibits pyro and piezoelectric properties, and it can be used as a particle sensor in laser ablation experiments. It was shown that the PVDF electric signal is proportional to the linear moment transferred by the plume to the sensor surface [25] and that the Time of Flight signal (TOF), when using this kind of sensor, is given by

$$S(t) \propto \frac{1}{t^5} \exp\left[-\frac{m}{2K_B T_z} \left(\frac{l}{t} - v_0 \right)^2 \right] \quad , (2)$$

where it was assumed a monoatomic beam and that the velocity distribution of the plume particles is given by a Maxwellian with a drift velocity v_0. In this

equation t is the time ellapsed since the beginning of the laser pulse, m is the particle mass, K_B is the Boltzmann constant and l is the distance between target and sensor. By fitting this equation to the PVDF sensor signal it is possible to obtain the drift velocity and the plume translational temperature. Fig. 3 shows a typical PVDF signal and the best fitting for Eq. (5).

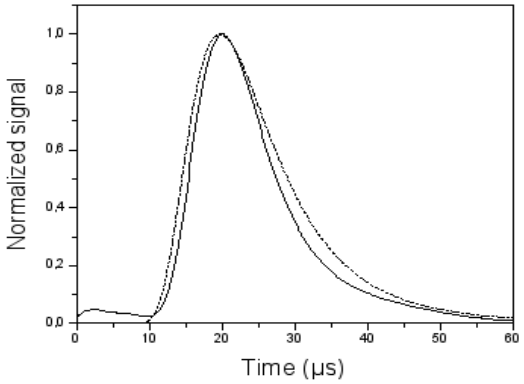

Figure 3: PVDF signal (solid line) and a best fit for the Eq. 5 (dashed line).

With a tungsten target it was obtained translational temperatures between 5×10^4 K and 8×10^4 K and drift velocities between 4.0×10^3 m/s and 6.5×10^3 m/s. These results are in the same range of the valaues obtained with metal ablation with excimer lasers [24]. For copper samples, the translational temperature is about 10^4 K and the drift velocity is about 10^3 m/s.

A 3 mm slit was attached to the PVDF sensor (that originally is 10 mm wide) and was moved across the plume in order to observe the plume directionality. Fig. 4 shows a plot of the peak PVDF sensor signal against the sensor distance from the plume axis. In order to have a figure of merit for the plume directionality, these results were fitted to a cosine law function $S(x) \propto \cos^n(x)$. For e-beam evaporated metals, for instance, n lies between 3 and 8 [26], whereas for our experiments, this fitted parameter was always larger than 40. It means that the plume is a very well collimated beam of particles.

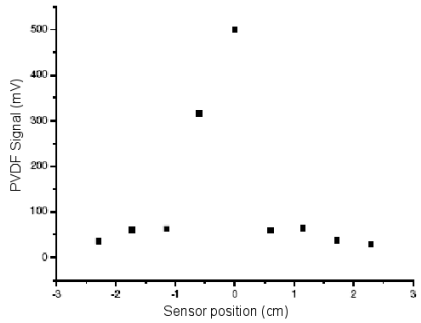

Figure 4: Angular distribution PVDF signal. The PVDF signal refers to the signal peak and the sensor position refers to the distance from the normal to the target surface. The distance between target and sensor was 150 mm.

6. Langmuir probe measurements

A Langmuir probe was used in order to obtain the plasma parameters. The Langmuir probe is a very well established method for plasma characterization and, in the particular case of expanding plume, it is necessary to follow the steps settled in the Refs. [27-29]. A 10 mm long and 250 μm diameter tungsten wire, supported by an alumina tube, was used as Langmuir probe. The probe was biased with different polarization voltages and its electric signal against time was recorded for further analysis. Fig. 5 shows a set of probe signals for different polarization voltages.

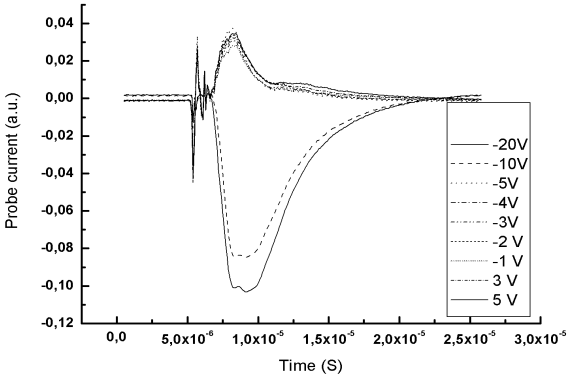

Figure 5: Langmuir probe electric current for different polarization voltages.

The peak probe current was plotted against polarization voltage, as shown in Fig. 6, and the traditional Langmuir probe analysis was performed. As well known, the plateau for negative voltages gives information about ion density, the inclination of the curve in the vicinity of the null voltage (when plotted in logarithmic scale) gives information about the electron temperature and the saturation of the function, for positive voltage, gives information about electron density. When working with tungsten, it was obtained electron temperature of about 30 eV, electron densities of about 10^{10} cm^{-3} and ion densities with the same order of magnitude. With copper, it was obtained densities (ion and electron) in the order of 10^{11} cm^3 and electron temperatures in the range 1-4 eV.

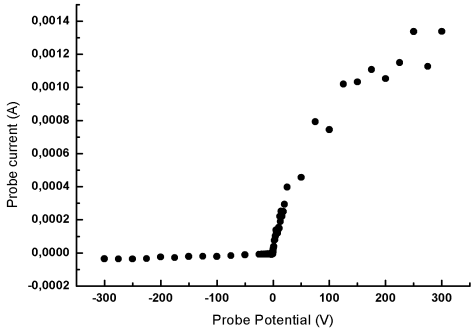

Figure 6: Typical Langmuir probe current polarization for the peak value of the signals shown in Fig. 5.

If the probe is negatively polarized, its electric signal can also be used in TOF analysis for ions. It must also be taken into account that the PVDF signal is proportional to linear momentum transfer whereas the Langmuir probe is proportional to the ion density. So, the TOF signal, for the Langmuir probe, must be written as

$$S(t) \propto \frac{1}{t^3} \exp\left[-\frac{m}{2 k_B T_T} \left(\frac{l}{t} - v_D \right)^2 \right] \quad (3)$$

like proposed in [30, 31].

The TOF analysis of the Langmuir probe signal resulted in the same figures obtained with the PVDF sensor, confirming those results.

7. Deposition rate analysis

Deposition rate measurements were accomplished in order to calibrate the PVDF sensor and to compare the neutrals and ions density. An Inficom XTM/2P quartz oscillator deposition sensor was used as measurement device. This sensor measures the accumulated deposited material, whereas the PVDF and the Langmuir probe are able to measure the densities during the plume duration. Supposing both the neutral and ion are monoatomic, the average particle density, in particles/cm^3, during the plume lifetime, can be estimated by

$$n_V = \frac{\dot{M}}{m \tau_P f v_0} \quad (4)$$

where $\dot{M}$ is the deposition rate measured by the sensor (in mass per time per area unity), m is the particle mass, τ_P is the plume lifetime, f is the repetition rate and v_0 is the plume velocity. Both τ_P and v_0 can be obtained from the TOF analysis. Such estimation, using the parameters obtained in the ablation of tungsten, gave a total particle density in the order of 10^{11} cm^3, which is only one order of magnitude larger than the ion density, obtained by using Langmuir probe. It is necessary to study the deposition rate of other materials yet, but it is reasonable to conclude that the neutral density and ion density, in the plume generated by the ablation of metal targets with copper lasers, are roughly in the same order of magnitude, that is about 10^{11} cm^{-3} for the tungsten.

8. Conclusions

Summarizing, the plume generated by laser ablation, using copper laser, has the following characteristics:

- mostly monoatomic, even for complex targets;
- extremely directional;
- densities about 10^{11} cm^{-3};
- electron temperature of tens eV
- drift velocity ~ 10^3 m/s;
- neutral and ion density about the same order of magnitude;
- tiny amounts.

So, as far as separation processes are concerned, the laser-ablation-generated-plume gives rise to some different ideas. The ablation itself can be considered as a separation method, because, departing from a complex target, a plume made of elementals is generated. A fraction of these elementals is neutral and the rest is ionized. If the ions are separated from the jet by electromagnetic traps, a jet made of neutrals is produced. The Laser Resonant Ionization can then be used as a specie discriminator for the neutrals, like in AVLIS [32]. The ions with energy in the range of 50 eV, in a very well collimated beam, that can be separated by using plasma separation methods [33]. One can even think about Laser Resonant Ionization of ions, instead of neutrals.

At IEAv there is an emerging program of isotope separation that intends to take monazitic sand as raw material, to separate it in its elementals by using laser ablation and separate rare earths by Laser Resonant Ionization. It is known that the amount of enriched material by this method will be small. However, the application that is predicted is the doping of waveguides in the research of photonic devices, that demands only tiny amount of doping materials.

9. Acknowledgments

The authors would like to thank Fundação de Amparo à Pesquisa do Estado de São Paulo (FAPESP) e à Coordenação de Aperfeiçoamento de Pessoal de Nível Superior (CAPES) for the financial support.

10. Bibliograpy

1 Maiman, T.H., Nature, **187**, 493, 1960.
2 Dubowski, J.J., et al., Superl. Microstruct. **9**, 327, 1991.
3 Dubowski, J.J., et al., Appl. Phys. Lett., **59**, 1591, 1991.
4 Yan, L., et al., Chinese Phys., **15**, 2271, 2006.
5 Günther, D., Spectroc. Acta B, **54**, 381, 1999.
6 Chang, J.J., et al., Proc. Laser Material Processing Conference, ICALEO'94, Orlando: Florida, 223, 1994.
7 Chang, J.J., et al., Appl. Phys. Lett., **69**, 473, 1996.
8 Smith, H.M., Turner, A.F., Appl. Opt., **4**, 147, 1965.
9 Groh, G., J. Appl. Phys., **39**, 5804, 1968.
10 G. Hass and J. B. Ramsey, Appl. Opt., **8**, 1115, 1969.
11 Ouchi H., et al.; Jpn. J. Appl. Phys., **31**, 1979, 1992.
12 Okoshi M., et al., Appl. Surf. Scienc., **154-155**, 424, 2000.
13 Chang, J.J., Warner, B.E., Appl. Phys. **69**, 473, 1996.
14 Rodrigues, N. A. S., et al., Applied Surface Science, **200**, 68, 2002.
15 P. P. Pronko, et. al., Phys. Rev. Lett., **83**, 2596, 1999.
16 Gupta, P.D., et al., J. Appl. Phys., **51**, 3422, 1980.
17 Destro, M., Published in this Proceedings.
18 Amoruso, S., et al., J. Phys. B, **32**, R131, 1999.
20 Kapitan, D., et al., CLEO-Europe, paper CThH75, 1998.
21 Capitelli, M., et al., Spectroch. Acta, **B 59**, 271, 2004.
22 Duley, W.W.; CO_2 lasers, effects and applications, Academic Press, N.Y., 1976.
23 Riva, R., et al., Proc. 5th Workshop on Separation Phenomena in Liquids and Gases, 1996, Foz do Iguaçu – Brazil, 241, 1996.
24 Amoruso, S., et al., Appl. Surf. Sc., **127-129**, 953, 1998.
25 Gião, M.A.P., et al., Review of Scientific Instruments, **75**, 5213, 2004.
26 Sciller, S.; Eigh, U.; Panzer, S.; *Electron beam technology*, John Wiley, New York, 1982.
27 Toftmann, B., Apl. Surf. Sc., **186**, 293, 2002.
29 Segall, S.B., et al., Phys. Rev., **16**, 1149, 1973.
30 Utterback, N.G., Phys. Fluids, **19**, 901, 1976.
31 Kools, J.C.S., J. Appl. Phys, **71**, 4547, 1992.
32 Schwab, C., et al., Prog. Nucl. En., **33**, 217, 1998.
33 Grossman, M.W., Shepp, T.A., IEEE Transaction on Plasma Science, **19**, 1114, 1991.